J Neural Transm (2009) 116:1243–1251
DOI 10.1007/s00702-009-0293-y

DEMENTIAS - ORIGINAL ARTICLE

Phosphorylation of soluble tau differs in Pick's disease and Alzheimer's disease brains

Janet van Eersel · Mian Bi · Yazi D. Ke · John R. Hodges · John H. Xuereb · Gillian C. Gregory · Glenda M. Halliday · Jürgen Götz · Jillian J. Kril · Lars M. Ittner

Received: 28 May 2009 / Accepted: 3 August 2009 / Published online: 20 August 2009

Abstract Frontotemporal lobar degeneration (FTLD) is a common cause of presenile dementia characterised by behavioural and language disturbances. Pick's disease (PiD) is a subtype of FTLD, which presents with intraneuronal inclusions consisting of hyperphosphorylated tau protein aggregates. Although Alzheimer's disease (AD) is also characterised by tau lesions, these are both histologically and biochemically distinct from the tau aggregates found in PiD. What determines the distinct characteristics of these tau lesions is unknown. As phosphorylated, soluble tau has been suggested to be the precursor of tau aggregates, we compared both the level and phosphorylation profile of tau in tissue extracts of AD and PiD brains to determine whether the differences in the tau lesions are reflected by differences in soluble tau. Levels of soluble tau were decreased in AD but not PiD. In addition, soluble tau was phosphorylated to a greater extent in AD than in PiD and displayed a different phosphorylation profile in the two disorders. Consistently, tau kinases were activated to different degrees in AD compared with PiD. Such differences in solubility and phosphorylation may contribute, at least in part, to the formation of distinct tau deposits, but may also have implications for the clinical differences between AD and PiD.

Keywords Alzheimer's disease · Frontotemporal lobar degeneration · ERK · Phosphorylation · Pick's disease · Tau

J. van Eersel · J. J. Kril
Discipline of Pathology, The University of Sydney, Sydney, NSW 2006, Australia

J. van Eersel · M. Bi · Y. D. Ke · J. Götz · L. M. Ittner (✉)
Alzheimer's and Parkinson's Disease Laboratory, Brain and Mind Research Institute, The University of Sydney, 100 Mallett Street, Camperdown, NSW 2050, Australia
e-mail: littner@med.usyd.edu.au

J. R. Hodges · G. C. Gregory · G. M. Halliday
Prince of Wales Medical Research Institute, The University of NSW, Barker Street, Randwick, NSW 2031, Australia

J. H. Xuereb
Department of Pathology, University of Cambridge, Cambridge, UK

J. Götz
The Medical Foundation, The University of Sydney, Camperdown, NSW 2050, Australia

J. J. Kril
Discipline of Medicine, The University of Sydney, Sydney, NSW 2006, Australia

Introduction

Alzheimer's disease (AD) is the most common cause of dementia, followed by frontotemporal lobar degeneration (FTLD), which typically presents before 65 years of age (Hodges et al. 2004). FTLD is an umbrella term for a heterogenous group of neurodegenerative disorders that are characterised by atrophy of the frontal and/or temporal lobes (Broe et al. 2003). Examples of FTLD include Pick's disease (PiD) and corticobasal degeneration. In contrast to AD, which presents predominantly with memory loss, FTLD is associated with changes in personal and social conduct, behaviour and language disturbances, and often motor symptoms (McKhann et al. 2001). AD and FTLD can also be differentiated histopathologically. In AD, neuronal loss is observed together with two hallmark lesions, β-amyloid plaques and tau-containing neurofibrillary

tangles (NFTs) (Goedert and Spillantini 2006). In FTLD however, neuronal loss is found together with lesions that typically consist of either aggregated tau or aggregated TAR DNA-binding protein of 43 kDa (TDP-43), in the absence of overt β-amyloid plaques (Cairns et al. 2007).

The microtubule-associated protein tau is a predominantly neuronal protein that, under physiological conditions, promotes and stabilises the assembly of microtubules (Lee et al. 2001). In neurodegenerative disorders with tau pathology it becomes hyperphosphorylated at both physiological and pathological sites (Ballatore et al. 2007). As a result, tau detaches from microtubules and becomes soluble. Furthermore, under normal physiological conditions, tau is primarily localized to axons, however, hyperphosphorylated and soluble tau redistributes to the somatodendritic compartment in AD, and the somatoaxonal compartment in PiD (Probst et al. 1996). Eventually, hyperphosphorylated tau forms fibrillar aggregates and assembles into insoluble deposits (Ballatore et al. 2007). Although in AD and PiD these deposits have similar ultrastructural characteristics, they can be clearly distinguished histologically (King et al. 2001). The intraneuronal tau deposits in AD present as flame-shaped NFTs, whereas the Pick bodies (PiB) that characterize PiD are typically round, intraneuronal inclusions (Kril and Halliday 2001; Uchihara et al. 2003). The question thus arises whether there are differences in the post-translational modification of soluble tau (Chen et al. 2004), such as phosphorylation, that could explain the differences in the tau pathology in AD and PiD.

Methods

Human brain tissue

Brain tissue was obtained from the National Neural Tissue Resource Centre, the Australian Brain Bank Network and the Cambridge Brain Bank as approved by the Human Ethics Review Committees of the Universities of Sydney and New South Wales. All procedures complied with the statement on human experimentation issued by the National Health and Medical Research Council of Australia. All persons gave their informed consent prior to their inclusion in the study. Frozen temporal cortex from four sporadic AD cases (age range 67–78, mean 72 ± 5; post-mortem delay 52 ± 24 h), four sporadic PiD cases (age range 62–75, mean 71 ± 6; post-mortem delay: 12 ± 5 h), and four control cases (age range 73–79, mean 76 ± 3; post-mortem delay 51 ± 11 h) was used for biochemical analysis (Table 1). For histology and immunohistochemistry, fixed tissue from an additional three sporadic AD cases (age range 67–83, mean 76 ± 8), three sporadic PiD cases (age range 63–71, mean 67 ± 4) and three control cases (age range 62–83, mean 73 ± 11) was used (Table 1). Controls were free from psychiatric, neurological or neuropathological diseases. None of the AD or PiD cases had a family history suggestive of an autosomal dominant disease.

Antibodies

Brain tissue was analysed with a range of phosphorylation-independent and -dependent antibodies. Total tau was detected using Tau-5 (Millipore, Billerica, MA, USA; amino acids 210–241). Specific tau phosphorylation sites were investigated using the following phosphorylation-dependent antibodies: AT270 to detect tau phosphorylated at Thr181 (Pierce, Rockford, IL, USA); AT8 for tau phosphorylated at Ser202/Thr205 (Pierce); AT100 for tau phosphorylated at Ser212/Thr214 (Pierce); AT180 for tau phosphorylated at Thr231/Ser235 (Pierce); 12E8 for tau phosphorylated at Ser262/Ser356 (Dr Peter Seubert, Elan Pharmaceuticals, South San Francisco, CA, USA); PHF-1 for tau phosphorylated at Ser396/Ser404 (Dr Peter Davies, Albert Einstein College of Medicine, Bronx, NY, USA) and pS422 for tau phosphorylated at

Table 1 Patient details

Diagnosis	Age (y)	Gender	Brain weight (g)	PMD (h)
Co	73	F	1,250	60
Co	77	F	1,336	36
Co	74	M	1,425	48
Co	79	M	1,448	60
Co[a]	83	F	1,275	24
Co[a]	75	M	1,306	44
Co[a]	62	M	1,334	10
AD	68	F	875	44
AD	75	F	1,206	80
AD	78	F	1,075	24
AD	67	M	1,235	60
AD[a]	67	F	1,140	23
AD[a]	83	M	1,071	36
AD[a]	77	F	1,345	48
PiD	62	F	1,150	12
PiD	73	F	1,120	4
PiD	72	F	900	16
PiD	75	F	810	15
PiD[a]	67	M	1,000	14
PiD[a]	63	F	1,060	5
PiD[a]	71	F	925	5

AD Alzheimer's disease, *Co* healthy control, *PiD* Pick's disease, *PMD* postmortem delay

[a] Denotes tissue used for immunohistochemical analysis

Ser422 (Invitrogen, Carlsbad, CA, USA). The following antibodies were used to determine kinase levels and activity: extracellular signal-regulated protein kinase (ERK)1/2, jun N-terminal kinase (JNK)1/2, phosphorylated JNK1/2 (all Sigma), phosphorylated ERK1/2 (Cell Signalling), GSK3β and S9 phosphorylated GSK3β (both Abcam). Glyceraldehyde-3-phosphate-dehydrogenase (GAPDH; Millipore) was used as loading control and to normalize Western blots (Hoerndli et al. 2004). For visualisation, alkaline phosphatase-coupled secondary antibodies to mouse and rabbit IgG and IgM (Sigma) were used for Western blotting, or biotinylated secondary antibodies to mouse and rabbit IgG (Vector Laboratories, Burlingame, CA, USA) for immunohistochemistry.

Histology and immunohistochemistry

Brains were removed at autopsy, weighed and the volume determined by fluid displacement following fixation for 14 days in 15% neutral buffered formalin. After removal of the cerebellum, the cerebrum was embedded in 3% agarose and sliced at 3 mm intervals. Tissue from the hippocampal formation at the level of the lateral geniculate nucleus region was sampled, embedded in paraffin and sectioned for further analysis. Bielschowsky and Gallyas silver stainings of paraffin sections were performed following standard procedures. Immunohistochemical analysis was carried out as previously described (Ittner et al. 2005a, 2005b). Briefly, 3 µm sections were rehydrated through a descending series of ethanol followed by antigen retrieval (except for detection with 12E8 and AT270) in citrate buffer (10 mM, pH 5.8) in an RHS-1 Microwave Vacuum Histoprocessor (Milestone Medical, Sorisole, Bergamo, Italy) at a final temperature of 120°C for 1 min. Sections were then treated with 3% hydrogen peroxide for 20 min to quench endogenous peroxidase activity. Non-specific binding sites were blocked by incubating the sections in blocking buffer (3% heat-inactivated normal goat serum, 2% bovine serum albumin (BSA), 0.1% Tween-20 in PBS) for 1 h at room temperature, followed by overnight incubation at 4°C with primary antibodies diluted in blocking buffer. The following primary antibody dilutions were used: PHF-1 (1:500), AT8 (1:250), 12E8 (1:5000), and AT270 (1:200). Sections were then incubated with biotinylated secondary antibodies (1:200) for 1 h at room temperature, visualised with Vectastain Elite-DAB Kit (Vector Laboratories, Burlingame, CA, USA) and counterstained with hematoxylin (Vector). After dehydration, coverslips were mounted with DPX Mountant (Sigma). To standardise the procedure, all staining was carried out simultaneously using Coverplates (Thermo Scientific, Waltham, MA, USA) and Sequenza slide racks (Thermo Scientific).

Protein extraction

Proteins were extracted from tissue samples as previously described (Goedert et al. 1992). Briefly, 1 g of temporal cortex was homogenised in 2 ml of RAB buffer (0.75 M NaCl, 100 mM 2-(*N*-morpholino) ethanesulphonic acid, 1 mM EGTA, 0.5 mM $MgSO_4$, 2 mM dithriothreitol at pH 6.8, containing protease inhibitors; Roche, Basel, Switzerland). Homogenates were incubated at 4°C for 20 min whilst shaking and then centrifuged at 11,000*g* for 20 min at 4°C. The supernatant was then centrifuged at 100,000*g* for 60 min at 4°C. The resulting supernatant was retained as the RAB-soluble protein fraction. For isolation of insoluble proteins, the pellets from the first and second spin were combined and resuspended in 10 ml (1:10w/v) of extraction buffer (10 mM Tris, 10% sucrose, 0.85 M NaCl, 1 mM EGTA, pH 7.4) and centrifuged at 15,000*g* for 20 min at 4°C. After centrifugation, the supernatant was retained and the pellet was re-extracted in 5 ml of extraction buffer and centrifuged at 15,000*g* for 20 min at 4°C. The supernatant was then collected and combined with the supernatant collected from the previous spin and treated with 1% sarkosyl for 1 h at room temperature while shaking. The supernatant was then centrifuged at 100,000*g* for 30 min at 4°C. The resulting supernatant was then removed and the pellet was resuspended in 50 mM Tris (pH 7.4, 0.2 ml/g of starting tissue), constituting the sarkosyl-insoluble protein fraction. Protein concentrations were determined using a BioRad DC Protein Assay kit (BioRad Laboratories, CA, USA) according to the manufacturer's instructions with a BioRad Benchmark Plus Microplate Spectrophotometer (BioRad Laboratories, CA, USA).

Western blots

Western blotting was performed as previously described (Ittner et al. 2005a). Between 10 and 40 µg of RAB-soluble protein or 2 µl aliquots of sarkosyl-insoluble proteins obtained by the extraction procedure described above were separated by 8% SDS-PAGE. The same controls were run with either the AD or PiD samples to enable comparison between blots. Proteins were electrophoretically transferred to nitrocellulose membranes (Hybond ECL Amersham, Rydalmere, NSW, Australia). For detection with AT8, AT100 or AT180 antibodies, antigen retrieval was performed following transfer by boiling the nitrocellulose membrane for 1 min in PBS buffer (10 mM sodium phosphate, 0.15 M NaCl, pH 7.5). Membranes were blocked with 5% (BSA in Tris-buffered saline with 0.1% Tween (TBS-T) at room temperature for 1 h, followed by incubation with the primary antibodies in 5% BSA/TBS-T/0.01% sodium azide overnight at 4°C whilst shaking.

Antibodies were used at the following dilutions: Tau-5 (1:2,000), AT270 (1:1,000), AT8 (1:1,000), AT100 (1:1,000), AT180 (1:1,000), 12E8 (1:1,000), PHF-1 (1:1,000), pS422 (1:1,000), ERK1/2 (1:1,000), phosphorylated ERK1/2 (1:1,000), JNK1/2 (1:1,000), phosphorylated JNK1/2 (1:1,000), GSK3β (1:1,000), phosphorylated GSK3β (1:1,000) and GAPDH (1:5,000). Subsequently, membranes were incubated with alkaline phosphatase-coupled secondary antibodies (1:15,000) in 1% BSA for 30 min at room temperature. Protein bands were visualised with Immobilon Chemiluminescent Alkaline Phosphatase substrate (Millipore, North Ryde, NSW, Australia) and detected in a VersaDoc Model 4000 CCD camera System (BioRad, Gladesville, NSW, Australia). To determine equal loading and for normalisation, membranes were stripped by washing in ddH_2O for 5 min, 0.2 M NaOH for 10 min and ddH_2O for 5 min and then probed for GAPDH. Quantification of bands was performed using BioRad Quantity One 1-D analysis software v4.6 (BioRad). Band intensities were normalized to individual GAPDH levels and then to Tau-5.

Statistics

Statistical analysis was conducted with GraphPad Prism 5.00 software (GraphPad Software, Inc., CA, USA). For comparisons, Student's *t* tests were used. All values are given as mean $\pm$ standard deviation (SD). A P value < 0.05 was taken as statistically significant.

Results

Differences in pathologic tau in AD and PiD brains

The major constituent of the intracellular lesions in AD and PiD is hyperphosphorylated tau (Buee et al. 2000). Here we analysed hippocampal sections from AD, PiD and control brains by immunohistochemistry using antibodies specific for various phosphorylation epitopes of tau, including AT270, AT8, AT100, AT180, 12E8, PHF-1 and pS422 (Fig. 1 and data not shown). In AD, PHF-1, AT8 and 12E8 stained NFTs, neuropil threads and plaque-associated dystrophic neurites throughout the CA1 and, less frequently, the dentate gyrus. Staining with AT270 showed a similar profile, albeit with a lower staining intensity. In PiD, ovoid-shaped inclusions consistent with PiBs stained with PHF-1, AT8 and intensely with AT270 but not with 12E8; these inclusions were found in pyramidal neurons of the CA1, and more frequently in neurons throughout the granular layer of the dentate gyrus. The absence of 12E8 immunoreactivity in PiD is a well-documented characteristic of the disorder (Bell et al. 2000; Probst et al. 1996).

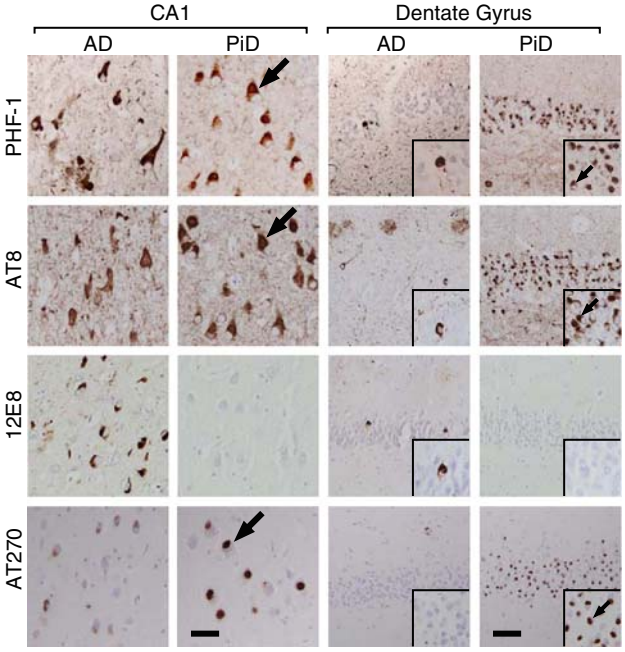

Fig. 1 Immunohistochemical analysis of tau phosphorylation in the CA1 sector and dentate gyrus of Alzheimer's disease (*AD*) and Pick's disease (*PiD*). Sections of the hippocampal CA1 region and dentate gyrus stained with phosphorylation-dependent antibodies to different epitopes of tau: PHF-1, AT8, 12E8 and AT270. In AD, PHF-1, AT8 and 12E8 show frequent staining of flame-shaped neurons in both the CA1 region and the dentate gyrus. A similar profile is seen with AT270, although with a lower staining intensity. In PiD, PHF-1 and AT8 show neuronal tau inclusions (*arrows*) in both the CA1 region and dentate gyrus. Staining with AT270 shows a similar profile, although with a greater staining intensity. Tau deposition in PiD is 12E8 negative, in agreement with previous findings. Insets show higher magnification of dentate gyrus neurons. No staining is found in controls (data not shown). *Scale bar* = 50 µm

Neuropil threads were also observed throughout the dentate gyrus and CA1 in PiD. No staining was observed in the controls (data not shown). Taken together, the histopathological analysis reveals neurofibrillary lesions and tau phosphorylation patterns that are distinct in AD and PiD.

Sarkosyl-insoluble tau in AD and PiD

Hyperphosphorylation of tau causes it to become prone to aggregation and eventually leads to the formation of insoluble intracellular deposits (Alonso et al. 2001). Sarkosyl extraction is routinely used to isolate and characterise insoluble tau from AD brain (Goedert et al. 1992). Here we used this method to compare tau solubility in four AD, four PiD and four control brains. When we analysed the sarkosyl-insoluble protein fractions by Western blotting using phosphorylation-independent and -dependent antibodies the antibody Tau-5 (total tau) revealed abundant sarkosyl-insoluble tau in both AD and PiD whereas minimal sarkosyl-insoluble tau was detected in the controls

(Fig. 2a, b). The phosphorylation-dependent antibodies PHF-1, AT8 and 12E8 (Fig. 2a, b), AT270, AT180, and pS422 (data not shown) revealed that sarkosyl-insoluble tau was phosphorylated at multiple sites in both AD and PiD brains. Taken together, we found abundant hyper-phosphorylated, sarkosyl-insoluble tau in both AD and PiD extracts, consistent with previous reports [reviewed in (Buee and Delacourte 1999)].

Differences in levels and phosphorylation profiles of soluble tau in AD and PiD

In the course of disease, progressive phosphorylation of soluble tau eventually leads to its deposition (Alonso et al. 1996). Furthermore, work in mice suggests an important role for soluble tau in neuronal dysfunction and memory impairment (Roberson et al. 2007; Santacruz et al. 2005). We speculated that alterations to soluble tau in AD and PiD may contribute to the formation of different tau lesions in these disorders. Therefore, we analysed and compared RAB-soluble protein preparations from four AD, four PiD and four control brains by Western blotting (Fig. 3a, b). We found that RAB-soluble tau levels were decreased in AD compared to controls and PiD, as revealed by Tau-5. Furthermore, Western blot analysis of RAB-soluble protein fractions with a range of phosphorylation-dependent tau antibodies showed that RAB-soluble tau was highly phosphorylated in both AD and PiD (Fig. 3c, d). Interestingly, phosphorylation of RAB-soluble tau was more pronounced at the PHF1 and pS422 epitopes when AD was

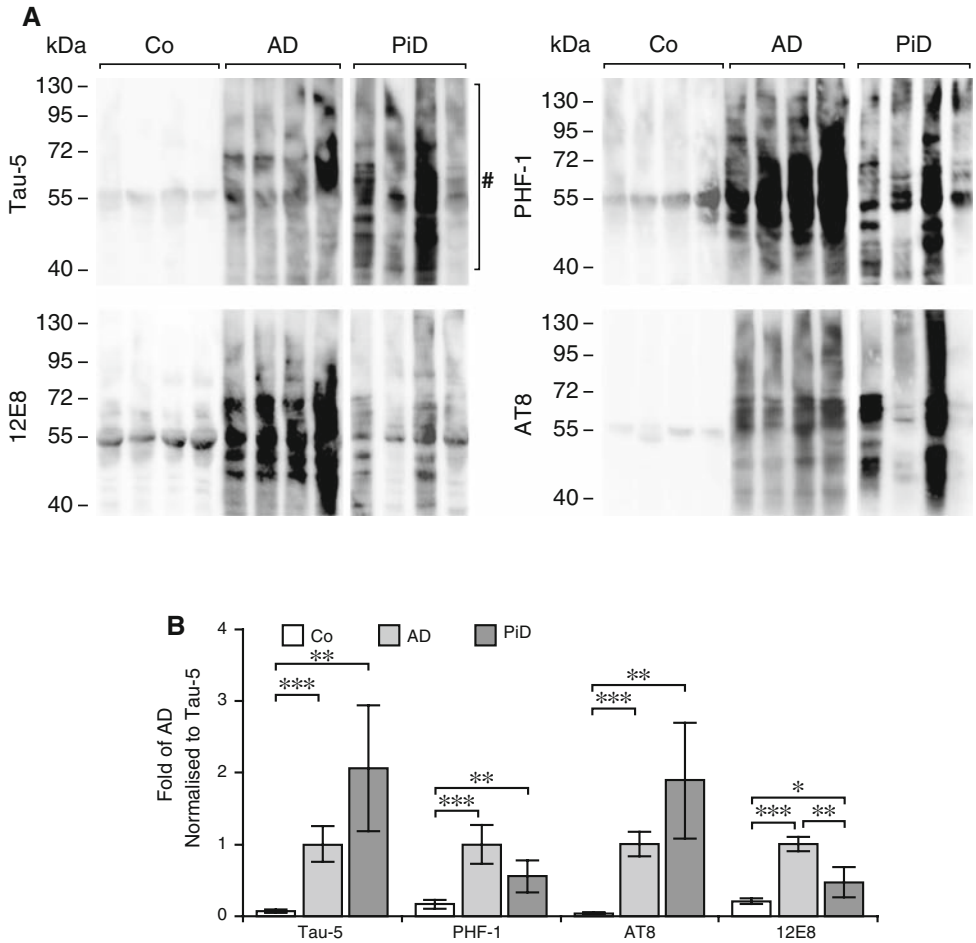

Fig. 2 Sarkosyl-insoluble tau in Alzheimer's disease (*AD*) and Pick's disease (*PiD*). **a** Sarkosyl-insoluble protein fractions, extracted from four control, four AD and four PiD brains, analysed by Western blotting using the phosphorylation-independent antibody to Tau-5, and the phosphorylation-dependent antibodies PHF-1, AT8 and 12E8. The hash indicates the range of bands used for quantification. **b** The band intensities are quantified and the results displayed as fold of AD. Levels of sarkosyl-insoluble tau are higher in AD and PiD brain extracts compared with controls. Although total levels of sarkosyl-insoluble tau (Tau-5) are greater in PiD, both AD and PiD preparations show similar degrees of phosphorylation at the PHF-1 and AT8 epitopes indicating a relatively greater amount of sarkosyl-insoluble tau phosphorylation in AD compared with PiD. Consistent with the immunohistochemistry (Fig. 2), 12E8 phosphorylation was only prominent in AD. Data are presented as mean ± SD. $^{*}P < 0.05$, $^{**}P < 0.01$, $^{***}P < 0.001$

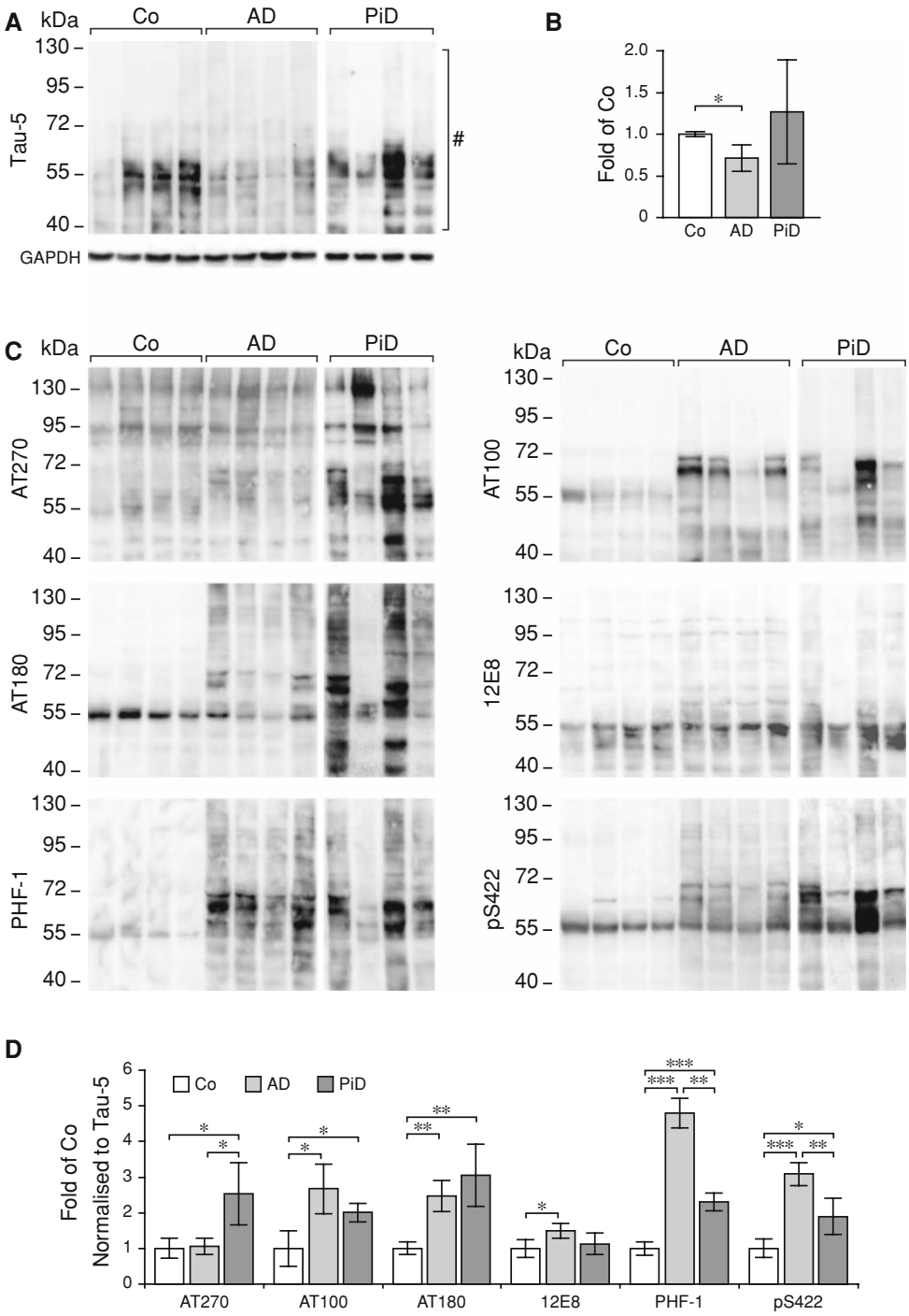

Fig. 3 Levels and phosphorylation of RAB-soluble tau extracted from Alzheimer's disease (*AD*) and Pick's disease (*PiD*) brains. **a** RAB-soluble protein fractions, extracted from four control, four AD and four PiD brains, analysed by Western blotting using the phosphorylation-independent antibody Tau-5. The hash indicates the range of bands used for quantification. **b** The band intensities are quantified, normalised against GAPDH levels, and results displayed as fold of control (Co) intensity. Levels of soluble tau detected with Tau-5 are comparable in PiD and control brains, but decreased in AD brains. **c** RAB-soluble protein fractions are analysed by Western blotting using the phosphorylation-dependent antibodies AT270, AT100, AT180, 12E8, PHF-1 and pS422. **d** The band intensities are quantified, normalised to GAPDH and total tau (Tau-5) levels and results displayed as fold of control intensity. RAB-Soluble tau is only prominently phosphorylated at the AT270 epitope in PiD. Data are presented as mean ± SD. $*P < 0.05$, $**P < 0.01$, $***P < 0.001$

compared with PiD, whereas the AT270 epitope was more prominent in PiD. Phosphorylation of RAB-soluble tau at the AT8 (data not shown), AT100 and AT180 epitopes was comparable in AD and PiD. In contrast, phosphorylation of RAB-soluble tau at the 12E8 epitope was generally lower in PiD than in AD, although it was slightly increased in AD compared to controls. Overall, the degree of phosphorylation was more variable in PiD than in AD.

Differently activated tau kinases in AD and PiD

Given the differences in RAB-soluble tau phosphorylation in AD and PiD, we next addressed whether there are also differences in the activity of tau kinases, using activation-dependent antibodies. Active ERK 1/2 was increased in AD and, even more so in PiD (Fig. 4a, b). In contrast, glycogen synthase kinase 3β (GSK3β) and c-JNK 1/2 (also

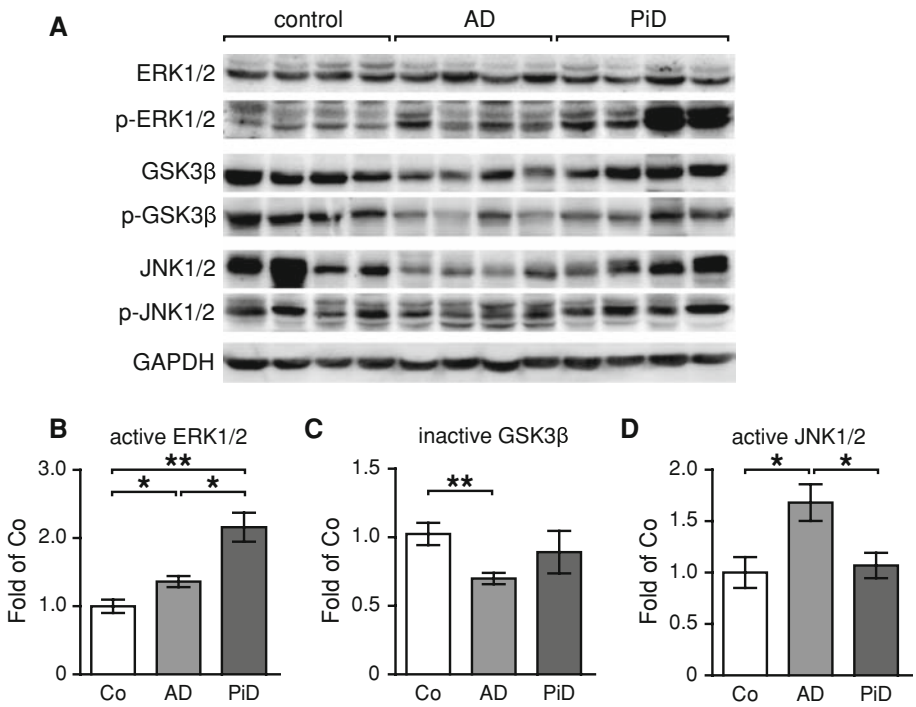

Fig. 4 Tau kinase activity is different in AD and PiD. **a** RAB-soluble protein fractions, extracted from four control, four AD and four PiD brains, were analysed by Western blotting using antibodies to ERK1/2, phosphorylated (p)-ERK1/2, GSK3β, p-GSK3β, JNK1/2, p-JNK1/2. GAPDH was detected to confirm equal loading. **b–d** The band intensities are quantified, normalised to GAPDH and the total kinase levels are displayed as fold of control (Co) intensity. Active ERK1/2 was increased in AD and even more so in PiD. In contrast, GSK3β and JNK1/2 only showed increased activation in AD. Data are presented as mean ± SD. $^{*}P < 0.05$, $^{**}P < 0.01$

termed stress-activated protein kinase 1) showed increased activation primarily in AD (Fig. 4a, c, d). Basal expression levels of these kinases were not different. Taken together, we show that RAB-soluble tau is phosphorylated at multiple sites in both AD and PiD, with distinct differences in the kinase activation and tau phosphorylation profiles (Table 2).

Table 2 Degree of phosphorylation at specific epitopes of RAB-soluble and sarkosyl-insoluble tau

Epitope	RAB-soluble tau		Sarkosyl-insoluble tau	
	AD	PiD	AD	PiD
AT270	+	+++	+++	+++
AT8	++	++	++	++
AT100	+++	++	n.a.	n.a.
AT180	+++	+++	++++	++
12E8	+	0	+++	+
PHF1	++++	++	++++	++
pS422	+++	++	++++	++

AD Alzheimer's disease, *PiD* Pick's disease, *n.a.* not analysed

Conclusion

Although the pathological hallmarks of AD and PiD both consist of hyperphosphorylated tau aggregates (Cairns et al. 2007), the flame-shaped NFTs of AD and the spherical PiBs of PiD appear remarkably different. Consistent with the criteria for AD and PiD diagnosis (Cairns et al. 2007), we found numerous intraneuronal lesions containing tau. As is typical for PiD, PiBs stained with all phospho-tau antibodies but 12E8 (Probst et al. 1996). Furthermore, analysis of sarkosyl-insoluble protein preparations with phosphorylation-dependent antibodies confirmed its hyperphosphorylation at multiple epitopes (not shown).

When tau becomes phosphorylated, its affinity for microtubules decreases, resulting in its detachment (Ballatore et al. 2007). Hyperphosphorylation of soluble tau may therefore represent the first step in a pathological cascade that leads to the deposition of tau (Buee et al. 2000). In this study, we show reductions in the levels of RAB-soluble tau from AD brains, consistent with previous findings (Ledesma et al. 1995; Zhukareva et al. 2003). This reduction may result from the recruitment of soluble tau to the insoluble pool, as suggested previously (Rizzu et al. 2000; Wang et al. 2007). Despite the reduction in RAB-soluble tau levels, overall tau levels are increased in AD, reflecting insoluble tau. In contrast to AD, levels of RAB-soluble tau in PiD and controls were comparable suggesting that in PiD sequestration of tau into the insoluble pool does not cause a reduction in the levels of soluble tau.

Despite lower levels of RAB-soluble tau in AD compared with PiD, RAB-soluble tau was more phosphorylated in AD than in PiD. However, one should take into account the higher post-mortem delay in our AD samples compared to PiD (52 vs. 12 h). Long post-mortem delays can lead to reduced phosphorylation of tau preparations (Ferrer et al.

2007). Hence, phosphorylation levels of RAB-soluble tau may be even higher in AD compared to PiD. In addition to differences in overall phosphorylation levels, phosphorylation of tau at particular sites discriminates AD and PiD. In AD, RAB-soluble tau is highly phosphorylated at the PHF-1 and pS422 epitopes compared to PiD, whereas the AT270 epitope displays more prominent phosphorylation in PiD compared to AD. Similarly, IHC showed intense AT270 staining of PiBs in PiD, while staining in AD was less pronounced. These site-specific differences may reflect differences in the balance of kinases and phosphatases that drive pathological phosphorylation of tau in AD and PiD (Chen et al. 2004). Whereas individual kinases and phosphatases in AD have been widely addressed, their roles in PiD remain to be elucidated (Gotz 2001). Consistent with previous reports (Pei et al. 1999, 2002), we show that several tau kinases display increased activity in AD, including ERK, GSK3β and JNK. Of those, only ERK was significantly activated in our PiD samples, even more than in AD. Whereas it has been suggested that the AT270 epitope of tau is predominantly phosphorylated by ERK, other sites are similarly phosphorylated by ERK and other kinases (Buee-Scherrer and Goedert 2002). Hence, it is possible that ERK is a driving tau kinase in PiD. Inhibitors of kinases such as GSK3, CDK5 and ERK, have emerged as promising drugs for the treatment of AD and related neurodegenerative disorders (Mazanetz and Fischer 2007). However, differences in kinase activation in AD and PiD may have to be considered in this therapeutic approach.

Taken together, levels of soluble tau are higher in PiD than in AD, whereas phosphorylation of soluble tau is more pronounced in AD. Although conclusions from small cohorts need to be made carefully, we show differences in soluble tau phosphorylation in AD vs PiD. This may contribute to the distinct histopathological characteristics of tau pathology in AD and PiD. Similar studies with larger cohorts are however needed. The relevance of soluble tau is supported by recent animal studies, which suggest that distinct soluble tau species, rather than the insoluble tau aggregates, cause neuronal dysfunction and degeneration (Gotz and Ittner 2008). Which tau form exerts the greatest neurotoxic effect remains to be elucidated.

Acknowledgments We thank Dr Vanessa Young for assistance with preparation of the tissue sections. Dr Peter Davies and Dr Peter Seubert generously provided antibodies. Tissues were received from the Australian Brain Donor Programs Prince of Wales Medical Research Institute Tissue Resource Centre, which is supported by the National Health and Medical Research Council of Australia and from the Cambridge Brain Bank. This research was supported by grants to J. Götz. from The University of Sydney, The Medical Foundation (University of Sydney), the National Health and Medical Research Council, Judith Jane Mason & Harold Stannett Williams Memorial Foundation, the Australian Research Council and New South Wales Government through the Ministry for Science and Medical Research (BioFirst Grant), and to L.M. Ittner from the Australian Research Council, the University of Sydney and the Deutsche Forschungsgesellschaft and the National Health and Medical Research Council (JK, LI, JG, GH). J. Götz is a Medical Foundation Fellow and G.M. Halliday is a National Health and Medical Research Council Principal Research Fellow. The authors declare that they have no conflict of interest.

References

Alonso AC, Grundke-Iqbal I, Iqbal K (1996) Alzheimer's disease hyperphosphorylated tau sequesters normal tau into tangles of filaments and disassembles microtubules. Nat Med 2:783–787

Alonso A, Zaidi T, Novak M, Grundke-Iqbal I, Iqbal K (2001) Hyperphosphorylation induces self-assembly of tau into tangles of paired helical filaments/straight filaments. Proc Natl Acad Sci USA 98:6923–6928

Ballatore C, Lee VM, Trojanowski JQ (2007) Tau-mediated neurodegeneration in Alzheimer's disease and related disorders. Nat Rev Neurosci 8:663–672

Bell K, Cairns NJ, Lantos PL, Rossor MN (2000) Immunohistochemistry distinguishes: between Pick's disease and corticobasal degeneration. J Neurol Neurosurg Psychiatry 69:835–836

Broe M, Hodges JR, Schofield E, Shepherd CE, Kril JJ, Halliday GM (2003) Staging disease severity in pathologically confirmed cases of frontotemporal dementia. Neurology 60:1005–1011

Buee L, Delacourte A (1999) Comparative biochemistry of tau in progressive supranuclear palsy, corticobasal degeneration, FTDP-17 and Pick's disease. Brain Pathol 9:681–693

Buee L, Bussiere T, Buee-Scherrer V, Delacourte A, Hof PR (2000) Tau protein isoforms, phosphorylation and role in neurodegenerative disorders. Brain Res Brain Res Rev 33:95–130

Buee-Scherrer V, Goedert M (2002) Phosphorylation of microtubule-associated protein tau by stress-activated protein kinases in intact cells. FEBS Lett 515:151–154

Cairns NJ, Bigio EH, Mackenzie IR, Neumann M, Lee VM, Hatanpaa KJ, White CL, Schneider JA, Tenenholz Grinberg L, Halliday GM et al (2007) Neuropathologic diagnostic and nosologic criteria for frontotemporal lobar degeneration: consensus of the consortium for frontotemporal lobar degeneration. Acta Neuropathol 114:5–22

Chen F, David D, Ferrari A, Gotz J (2004) Posttranslational modifications of tau—role in human tauopathies and modeling in transgenic animals. Curr Drug Targets 5:503–515

Ferrer I, Santpere G, Arzberger T, Bell J, Blanco R, Boluda S, Budka H, Carmona M, Giaccone G, Krebs B et al (2007) Brain protein preservation largely depends on the postmortem storage temperature: implications for study of proteins in human neurologic diseases and management of brain banks: a BrainNet Europe Study. J Neuropathol Exp Neurol 66:35–46

Goedert M, Spillantini MG (2006) A century of Alzheimer's disease. Science 314:777–781

Goedert M, Spillantini MG, Cairns NJ, Crowther RA (1992) Tau proteins of Alzheimer paired helical filaments: abnormal phosphorylation of all six brain isoforms. Neuron 8:159–168

Gotz J (2001) Tau and transgenic animal models. Brain Res Brain Res Rev 35:266–286

Gotz J, Ittner LM (2008) Animal models of Alzheimer's disease and frontotemporal dementia. Nat Rev Neurosci 9:532–544

Hodges JR, Davies RR, Xuereb JH, Casey B, Broe M, Bak TH, Kril JJ, Halliday GM (2004) Clinicopathological correlates in frontotemporal dementia. Ann Neurol 56:399–406

Hoerndli FJ, Toigo M, Schild A, Gotz J, Day PJ (2004) Reference genes identified in SH-SY5Y cells using custom-made gene

arrays with validation by quantitative polymerase chain reaction. Anal Biochem 335:30–41

Ittner LM, Koller D, Muff R, Fischer JA, Born W (2005a) The N-terminal extracellular domain 23–60 of the calcitonin receptor-like receptor in chimeras with the parathyroid hormone receptor mediates association with receptor activity-modifying protein 1. Biochemistry 44:5749–5754

Ittner LM, Wurdak H, Schwerdtfeger K, Kunz T, Ille F, Leveen P, Hjalt TA, Suter U, Karlsson S, Hafezi F et al (2005b) Compound developmental eye disorders following inactivation of TGFbeta signaling in neural-crest stem cells. J Biol 4:11

King ME, Ghoshal N, Wall JS, Binder LI, Ksiezak-Reding H (2001) Structural analysis of Pick's disease-derived and in vitro-assembled tau filaments. Am J Pathol 158:1481–1490

Kril JJ, Halliday GM (2001) Alzheimer's disease: its diagnosis and pathogenesis. Int Rev Neurobiol 48:167–217

Ledesma MD, Avila J, Correas I (1995) Isolation of a phosphorylated soluble tau fraction from Alzheimer's disease brain. Neurobiol Aging 16:515–522

Lee VM, Goedert M, Trojanowski JQ (2001) Neurodegenerative tauopathies. Annu Rev Neurosci 24:1121–1159

Mazanetz MP, Fischer PM (2007) Untangling tau hyperphosphorylation in drug design for neurodegenerative diseases. Nat Rev Drug Discov 6:464–479

McKhann GM, Albert MS, Grossman M, Miller B, Dickson D, Trojanowski JQ, Work Group on Frontotemporal Dementia, Pick's Disease (2001) Clinical and pathological diagnosis of frontotemporal dementia: report of the Work Group on Frontotemporal Dementia and Pick's Disease. Arch Neurol 58:1803–1809

Pei JJ, Braak E, Braak H, Grundke-Iqbal I, Iqbal K, Winblad B, Cowburn RF (1999) Distribution of active glycogen synthase kinase 3beta (GSK-3beta) in brains staged for Alzheimer disease neurofibrillary changes. J Neuropathol Exp Neurol 58:1010–1019

Pei JJ, Braak H, An WL, Winblad B, Cowburn RF, Iqbal K, Grundke-Iqbal I (2002) Up-regulation of mitogen-activated protein kinases ERK1/2 and MEK1/2 is associated with the progression of neurofibrillary degeneration in Alzheimer's disease. Brain Res Mol Brain Res 109:45–55

Probst A, Tolnay M, Langui D, Goedert M, Spillantini MG (1996) Pick's disease: hyperphosphorylated tau protein segregates to the somatoaxonal compartment. Acta Neuropathol 92:588–596

Rizzu P, Joosse M, Ravid R, Hoogeveen A, Kamphorst W, van Swieten JC, Willemsen R, Heutink P (2000) Mutation-dependent aggregation of tau protein and its selective depletion from the soluble fraction in brain of P301L FTDP-17 patients. Hum Mol Genet 9:3075–3082

Roberson ED, Scearce-Levie K, Palop JJ, Yan F, Cheng IH, Wu T, Gerstein H, Yu GQ, Mucke L (2007) Reducing endogenous tau ameliorates amyloid beta-induced deficits in an Alzheimer's disease mouse model. Science 316:750–754

Santacruz K, Lewis J, Spires T, Paulson J, Kotilinek L, Ingelsson M, Guimaraes A, DeTure M, Ramsden M, McGowan E et al (2005) Tau suppression in a neurodegenerative mouse model improves memory function. Science 309:476–481

Uchihara T, Ikeda K, Tsuchiya K (2003) Pick body disease and Pick syndrome. Neuropathology 23:318–326

Wang YP, Biernat J, Pickhardt M, Mandelkow E, Mandelkow EM (2007) Stepwise proteolysis liberates tau fragments that nucleate the Alzheimer-like aggregation of full-length tau in a neuronal cell model. Proc Natl Acad Sci USA 104:10252–10257

Zhukareva V, Sundarraj S, Mann D, Sjogren M, Blenow K, Clark CM, McKeel DW, Goate A, Lippa CF, Vonsattel J-P et al (2003) Selective reduction of soluble tau proteins in sporadic and familial frontotemporal dementias: an international follow-up study. Acta Neuropathol 105:469–476